

**University of Massachusetts Amherst**

---

**From the Selected Works of Derek Lovley**

---

December 28, 2012

# Molecular Analysis of the In Situ Growth Rate of Subsurface Geobacter Species

Dawn E. Holmes

Ludovic Giloteaux

Melissa Barlett

Milind A. Chavan

Jessica A. Smith, *University of Massachusetts - Amherst, et al.*



Available at: [https://works.bepress.com/derek\\_lovley/365/](https://works.bepress.com/derek_lovley/365/)

1 **Molecular Analysis of the *In Situ* Growth Rate of Subsurface *Geobacter* Species**

2 Dawn E. Holmes\*<sup>1</sup>, Ludovic Giloteaux<sup>2</sup>, Melissa Barlett<sup>2</sup>, Milind A. Chavan<sup>2</sup>, Jessica A.  
3 Smith<sup>2</sup>, Kenneth H. Williams<sup>3</sup>, Michael Wilkins<sup>3</sup>, Philip Long<sup>4</sup>, and Derek R. Lovley<sup>2</sup>

4 <sup>1</sup>Department of Physical and Biological Sciences, Western New England University,  
5 Springfield, MA 01119

6 <sup>2</sup>Department of Microbiology, University of Massachusetts, Amherst, MA 01003

7 <sup>3</sup>Department of Environmental Science, Policy and Management, University of  
8 California Berkeley, Berkeley, CA 94720

9 <sup>4</sup>Pacific Northwest National Laboratory, Richland, WA

10 Keywords: *Geobacter*, growth rate, microarray, gene expression, uranium bioremediation

11 Running title: Estimation of growth rate with qRT-PCR

12 \*Corresponding author:

13 Department of Physical and Biological Sciences

14 Western New England College

15 1215 Wilbraham Road

16 Springfield, MA 01119

17 Phone: (413) 577-0447

18 Fax: (413) 545-1578

19 **Email:** [dholmes@microbio.umass.edu](mailto:dholmes@microbio.umass.edu)

20 **Abstract**

21 Molecular tools that can provide an estimate of the *in situ* growth rate of *Geobacter*  
22 species could improve understanding of dissimilatory metal reduction in a diversity of  
23 environments. Whole genome microarray analyses of the subsurface isolate, *Geobacter*  
24 *uraniireducens*, grown under a variety of conditions identified a number of genes that are  
25 differentially expressed at different specific growth rates. Expression of two genes  
26 encoding ribosomal proteins, *rpsC* and *rplL*, were further evaluated with quantitative  
27 reverse transcription PCR (qRT-PCR) in cells with doubling times ranging from 6.56 h to  
28 89.28 h. Transcript abundance of *rpsC* correlated best ( $r^2= 0.90$ ) with specific growth  
29 rates. Therefore, expression patterns of *rpsC* were used to estimate specific growth rates  
30 of *Geobacter* species during an *in situ* uranium bioremediation field experiment in which  
31 acetate was added to the groundwater to promote dissimilatory metal reduction. Initially,  
32 increased availability of acetate in the groundwater resulted in higher expression of  
33 *Geobacter rpsC* and the increase in the number of *Geobacter* cells estimated with  
34 fluorescent *in situ* hybridization compared well with specific growth rates estimated from  
35 levels of *in situ rpsC* expression. However, in later phases cell number increases were  
36 substantially lower than predicted from *rpsC* transcript abundance. This change  
37 coincided with a bloom of protozoa and increased attachment of *Geobacter* species to  
38 solid phases. These results suggest that monitoring *rpsC* expression may better reflect the  
39 actual rate that *Geobacter* species are metabolizing and growing during *in situ* uranium  
40 bioremediation than changes in cell abundance.

41

42

43 **Introduction**

44           Understanding how environmental factors control the growth of microorganisms  
45 is a major goal in subsurface ecology. However, measuring the growth rate of bacterial  
46 populations *in situ* is challenging and approaches focused on enumeration of cells *in situ*  
47 are often inaccurate. Not only can unknown proportions of cells be attached to subsurface  
48 sediments, cell losses due to predation by protozoa or cell lysis by bacteriophage can also  
49 mask true rates of cell multiplication (1, 2).

50           A number of different techniques have been used to assess microbial growth rates  
51 in natural environments. For example, *in situ* growth rates can be estimated from the  
52 incorporation of radiolabeled thymidine or leucine into biomass (3, 4), or by the viable  
53 plate count technique (5). However, these approaches require sample incubation. Another  
54 approach that does not require sample incubation involves monitoring fluorescently  
55 labeled cells that are introduced into the subsurface (6, 7). This approach is limited to  
56 those strains that can readily be cultivated in the laboratory (8, 9), and studies have  
57 shown that labeled cells can become too diluted once substantial growth begins for  
58 results to be reliable (7).

59           *In situ* growth rates can also be estimated by quantifying the proportion of cells  
60 from the environment that are visually dividing with the frequency of dividing cells  
61 (FDC) technique (10, 11). This approach assumes that the duration of cell division ( $T_d$ )  
62 and chromosome replication is constant and identical for all individuals within a  
63 population and that all of the cells in a population are metabolically active. However,  
64 studies have shown that  $T_d$  values and chromosome replication rates can not only vary  
65 between different species but even within different strains of the same species (12, 13),

66 and cells in stationary or death phase will not be as metabolically active as those in  
67 logarithmic phase.

68 A potentially powerful technique for evaluating the physiological status and rates  
69 of activity of microorganisms in the subsurface is quantifying key gene transcripts (14).  
70 This approach has been particularly successful for monitoring *Geobacteraceae* species,  
71 which have physiological features that favor their growth in the subsurface (15-17) and  
72 have been found to be the predominant organisms associated with the anaerobic *in situ*  
73 bioremediation of groundwater contaminated with organic compounds or uranium (18).  
74 In such environments, it has been possible to determine with gene transcript analysis  
75 whether *Geobacteraceae* species are limited for major nutrients, such as ammonium and  
76 phosphate, as well as nutrients particularly important to *Geobacteraceae* species, such as  
77 iron (19-23). Furthermore, this method was used to determine whether *in situ*  
78 *Geobacteraceae* were experiencing oxidative or heavy metal stress (20, 24), and to  
79 estimate relative rates of *in situ* metabolism (25, 26). Here we report on a method for  
80 elucidating *in situ* growth rates of subsurface *Geobacteraceae* populations from gene  
81 transcript abundance.

## 82 **Materials and Methods**

### 83 **Growth of *Geobacter uraniireducens*.**

84 *Geobacter uraniireducens* strain RF4 (ATCC BAA-1134) was obtained from our  
85 laboratory culture collection. Cells were grown with acetate (5 mM) as an electron donor  
86 and either fumarate (40 mM), amorphous Fe(III) oxyhydroxide (100 mM), Mn(IV) oxide  
87 (20 mM), or sediments collected from a uranium-contaminated aquifer located in Rifle,  
88 Colorado, provided as an electron acceptor. All cultures except the sediment incubations

89 were grown in a bicarbonate-buffered, defined medium (27). All incubations were done  
90 in the dark under N<sub>2</sub>:CO<sub>2</sub> (80:20).

91 For sediment incubations, 40 g of heat-sterilized sediments, 6 mL groundwater,  
92 and acetate (5 mM) were added to 60 mL serum bottles in an anaerobic chamber under a  
93 N<sub>2</sub> atmosphere (28). Cells that served as an inoculum (2%) for sediment incubations  
94 were first grown in medium with acetate (5 mM) provided as an electron donor and  
95 amorphous Fe(III) oxyhydroxide (100 mM) provided as an electron acceptor. Growing  
96 *G. uraniireducens* in chemostats with soluble electron acceptors such as Fe(III) citrate or  
97 fumarate as previously described for *G. sulfurreducens* (29) was not feasible because *G.*  
98 *uraniireducens* cannot grow with Fe(III) citrate (30) and fumarate can be fermented when  
99 other electron donors are limiting. Therefore, in order to achieve a wide range of specific  
100 growth rates, *G. uraniireducens* was grown in batch cultures with acetate as the electron  
101 donor and a variety of electron acceptors (sediment Fe(III) oxides; synthetic Fe(III) or  
102 Mn(IV) oxides; or fumarate) at various temperatures (Supplementary Material, Figure  
103 S1A-D). Cell counts and the exponential growth equation ( $\mu = (\ln N_f - \ln N_o)/(t_f - t_o)$ ,  
104 where N<sub>o</sub> and N<sub>f</sub> are bacterial abundances at the beginning and end points) were used to  
105 determine specific growth rates for all pure culture studies of *G. uraniireducens*.

#### 106 **Site and description of field site.**

107 In 2010, a small-scale *in situ* bioremediation experiment was conducted on the  
108 grounds of a former uranium ore processing facility in Rifle, Colorado during the months  
109 of August-October. This site, designated the Old Rifle site, is part of the Uranium Mill  
110 Tailings Remedial Action (UMTRA) program of the U.S. Department of Energy. The  
111 test plot was adjacent to a previously studied larger experimental plot at the site (31). The

112 monitoring array consisted of 9 down-gradient and 6 injection wells (Supplementary  
113 Material, Figure S2). Groundwater for the experiment was collected from well CD-04.

114 During the field experiment, a concentrated acetate/bromide solution (50/20 mM)  
115 mixed with native groundwater was injected into the subsurface to provide approximately  
116 5 mM acetate to the groundwater over the course of 30 days as previously described (31,  
117 32). Bromide was utilized as a non-reactive tracer.

#### 118 **Analytical techniques.**

119 Acetate and fumarate concentrations were determined with an HP series 1100  
120 high-pressure liquid chromatograph (Hewlett Packard, Palo Alto, California) with a Fast  
121 Acid Analysis column (Bio-Rad laboratories, Hercules, California), an eluent of 8 mM  
122 H<sub>2</sub>SO<sub>4</sub> and an absorbance detection at 210 nm as previously described (31).

123 Fe(III) reduction in the Fe(III) oxide grown cultures was monitored by measuring  
124 the formation of Fe(II) over time with a ferrozine assay in a split-beam dual-detector  
125 spectrophotometer (Spectronic Genosys2; Thermo Electron Corp., Mountain View, CA)  
126 at an absorbance of 562 nm after a one hour extraction with 0.5 N HCl (27, 33). Fe(III)  
127 reduction in the sediments was monitored by first measuring Fe(II) in the sediments that  
128 could be extracted in 0.5 M HCl after a 1 hour incubation with a ferrozine assay (33).  
129 The remaining Fe(III) in the sediments that was not HCl-extractable was then converted  
130 to Fe(II) by the addition of 0.25 M hydroxylamine) (33). After addition of  
131 hydroxylamine, samples were incubated for an additional hour, and then measured with a  
132 ferrozine assay. The percentage of Fe(II) in the sediments was then determined by  
133 dividing the HCl-extractable Fe(II) by the hydroxylamine extractable Fe(II).

134 Cell numbers from pure cultures were determined by counting acridine orange  
135 stained cells with fluorescence microscopy on a Nikon Eclipse E600 microscope (34).

#### 136 **FISH and DAPI counts**

137 The microbial community was analyzed for *Geobacteraceae* and total bacteria  
138 using fluorescent *in situ* hybridization (FISH) and nucleic acid staining with 4',6-  
139 diamidino-2-phenylindole (DAPI). The number of *Geobacteraceae* was determined by  
140 the number of cells that hybridized to the following probes: GEO3A, GEO3B, and  
141 GEO3C (35). Groundwater samples were immediately fixed in a solution consisting of  
142 4% paraformaldehyde/0.5X phosphate buffered saline (PBS; Na<sub>2</sub>HPO<sub>4</sub>). This solution  
143 was vortexed for five seconds before being added to 0.2 μm white polycarbonate filters  
144 (GTTP; Millipore, Billerica, MA) and washed with 1% Nonidet (Sigma) solution.

145 Cells were hybridized for three hours as described previously (36) with a mix of  
146 probes GEO3A, GEO3B, and GEO3C in hybridization buffer (0.02 M Tris, 0.9 M NaCl,  
147 0.02% SDS) with a formamide concentration of 30% (v/v) at 46 °C (37). Filters were  
148 washed twice with wash buffer (0.02 M Tris, 0.1 M NaCl, 5 mM EDTA, 0.01% SDS)  
149 and incubated at 48 °C for 10 minutes. Filters were washed a final time with filtered,  
150 autoclaved, distilled water, placed on slides where they were embedded in Vectashield  
151 with DAPI (Vector Laboratories, Burlingame, CA) and observed with a Nikon  
152 epifluorescence microscope. Ten to twenty fields of view for each sample were  
153 enumerated; DAPI and FISH were both counted for each field. The DAPI and FISH  
154 staining efficiency for Rifle groundwater samples ranged from 68-79% and standard  
155 deviations among triplicate counts varied between 10-30% of the average number of  
156 cells.



157 **Extraction of RNA from samples**

158 For extraction of RNA from batch cultures, 100 ml of *G. uraniireducens* were  
159 first split into 50 ml conical tubes (Falcon), and pelleted by centrifugation at 3,600 x g for  
160 15 min.

161 RNA was extracted from sediment incubations when 75% of the total iron present  
162 in the sediments was reduced to Fe(II). Groundwater and sediment from the incubations  
163 (40 g sediment and 6 ml groundwater) were transferred into 50 ml conical tubes (Falcon),  
164 and pelleted by centrifugation at 3,600 x g for 15 min. Pellets were then immediately  
165 frozen in a dry ice, ethanol bath and stored at  $-80^{\circ}\text{C}$ . RNA was extracted from these  
166 pellets as previously described (19).

167 RNA was also extracted from groundwater collected from the U(VI)  
168 contaminated aquifer during the bioremediation field experiment. In order to obtain  
169 sufficient biomass from the groundwater for RNA extraction, it was necessary to  
170 concentrate 15 liters of groundwater by impact filtration on 293 mm diameter Supor  
171 membrane disc filters with a pore size of  $0.2\ \mu\text{m}$  (Pall Life Sciences), which took about 3  
172 minutes. All filters were placed into whirl-pack bags, flash frozen in a dry ice/ethanol  
173 bath, and shipped back to the laboratory where they were stored at  $-80^{\circ}\text{C}$ . RNA was  
174 extracted from filters as previously described (19).

175 High quality RNA was extracted from the groundwater, sediment, and batch  
176 culture samples. In order to ensure that RNA samples were not contaminated with DNA,  
177 PCR amplification with primers targeting the 16S rRNA gene was conducted on RNA  
178 samples that had not undergone reverse transcription.

179 **Microarray analysis**

180 The MessageAmp II- Bacteria Kit (Ambion) was used to amplify total RNA (0.5  
181 µg) according to the manufacturers instructions. Amplified RNA was then chemically  
182 labeled with Cy3 (for the control or soluble electron acceptor condition) or Cy5 (for the  
183 experimental insoluble condition) dye using the MicroMax ASAP RNA Labeling Kit  
184 (Perkin Elmer, Wellesley, MA) according to the manufacturer's instructions.

185 Customarray™ 12K oligonucleotide microarrays (Combimatrix, Mukilteo, WA)  
186 were designed from the genomic sequence of *G. uraniireducens* (accession number  
187 [NZ\\_AAON00000000](#)). A complete record of all oligonucleotide sequences used and raw  
188 and statistically treated data files is available in the NCBI Gene Expression Omnibus  
189 database (GEO data series GSE10920 and GSE12874).

190 Results were analyzed via LIMMA mixed model algorithms as previously  
191 described (38-41) and multiple oligonucleotide probes were analyzed from each gene (3  
192 or 4 probes per gene). A gene was only considered differentially expressed if at least half  
193 of the probes had p values less than or equal to 0.01.

194 **Testing and design of primers**

195 Before primers for quantitative reverse transcription PCR (qRT-PCR) targeting *in*  
196 *situ rpsC* and *proC* mRNA transcripts could be designed, cDNA libraries were  
197 constructed with products amplified from RNA extracted from groundwater with the  
198 degenerate PCR primer sets, Geo\_rpsC200f/640r and Geo\_proC55f/460r (Supplementary  
199 Material Table S1). These degenerate primers were designed from nucleotide and amino  
200 acid sequences extracted from the following *Geobacteraceae* genomes: *G.*  
201 *sulfurreducens*, *G. metallireducens*, strain FRC-32, strain M21, *G. uraniireducens*, *G.*

202 *lovleyi*, and *G. bemidjensis*. Genome sequence data were obtained from the DOE Joint  
203 Genome Institute (JGI) website ([www.jgi.doe.gov](http://www.jgi.doe.gov)). Products from these degenerate  
204 primer sets were cloned into the TOPO TA cloning vector, version M (Invitrogen,  
205 Carlsbad, CA). One hundred plasmid inserts from both the *rpsC* and *proC* cDNA  
206 libraries were sequenced with the M13F primer at the University of Massachusetts  
207 Sequencing Facility. A *Geobacter rpsC* sequence accounted for 85% of the sequences in  
208 the *rpsC* cDNA library and a *Geobacter proC* sequence accounted for 90% of the *proC*  
209 cDNA library. Both of these dominant sequences were used to design qRT-PCR primers  
210 specific for *in situ* *Geobacter* species present during bioremediation.

211 All qRT-PCR primers were designed according to the manufacturer's  
212 specifications (Applied Biosystems) and had amplicon sizes ranging from 100-200 bp.  
213 Pure culture primers designed for qRT-PCR only targeted *G. uraniireducens* cells.  
214 GU\_rpsC178f/245r, GU\_rplL66f/136r, and GU\_proC263f/367r primer sets were used to  
215 quantify *rpsC*, *rplL*, and *proC* mRNA transcripts from *G. uraniireducens* and  
216 Geo\_rpsC50f/147r and Geo\_proC13f/140r targeted *rpsC* and *proC* cDNA made from  
217 RNA extracted from groundwater (Supplementary Material Table S1).

218 The reference gene, *proC*, which appears to be constitutively expressed by  
219 *Geobacteraceae* species in pure cultures and in the environment (22, 24, 42) and was not  
220 differentially expressed in any of the microarray experiments from this study, was  
221 selected as an external control. The gene *proC* encodes pyrroline-5-carboxylate  
222 reductase, which is involved in arginine and proline metabolism. In order to further  
223 confirm the fact that *proC* expression is constitutive, *proC* mRNA transcript abundance  
224 was compared to biomass harvested from *G. uraniireducens* cultures grown at four

225 different temperatures with acetate as the electron donor and fumarate as the electron  
226 acceptor. All four of these cultures were harvested at an  $OD_{600\text{ nm}}$  of 0.3 (biomass *ca.* 49  
227 mg protein/L), and the number of *proC* mRNA transcripts in these samples only varied  
228 from  $1.66 \times 10^5$  to  $3.34 \times 10^5$ .

229 Expression by one growth-related and one reference gene was monitored in this  
230 study and results indicated that mRNA transcripts from these genes could be used to  
231 reliably predict *in situ* growth. However, in order to better understand total cell activity,  
232 future studies might want to target expression profiles of more genes.

### 233 **PCR amplification parameters and clone library construction**

234 A DuraScript enhanced avian RT single strand synthesis kit (Sigma) was used to  
235 generate cDNA as previously described (19). Previously described parameters were used  
236 to amplify genes of interest with degenerate primers (43).

237 For construction of 16S rRNA gene clone libraries, gene fragments were first  
238 amplified by PCR with the following primer sets; 8F (44) with 519R (45) and 338F (46)  
239 with 907R (45). PCR products were purified with the Gel Extraction Kit (Qiagen), and  
240 clone libraries were constructed with a TOPO TA cloning kit, version M (Invitrogen,  
241 Carlsbad, CA) according to the manufacturer's instructions.

### 242 **Quantification of gene expression by qRT-PCR.**

243 Once the appropriate cDNA fragments were generated by RT-PCR, quantitative  
244 PCR amplification and detection were performed with the 7500 Real Time PCR System  
245 (Applied Biosystems). Optimal qRT-PCR conditions were determined using the  
246 manufacturer's guidelines; 50 cycles of 95°C for 15 seconds and 60°C for 1 minute.

247 Each PCR mixture consisted of a total volume of 25  $\mu$ L and contained 1.5  $\mu$ L of  
248 the appropriate primers (stock concentrations, 15  $\mu$ M), 5 ng cDNA, and 12.5  $\mu$ L Power  
249 SYBR Green PCR Master Mix (Applied Biosystems). Standard curves covering 8 orders  
250 of magnitude were constructed with serial dilutions of known amounts of purified cDNA  
251 quantified with a NanoDrop ND-1000 spectrophotometer at an absorbance of 260 nm.

252 The qPCR efficiency (95% to 99%) was calculated based on the slope of the  
253 standard curve. All qPCR assays had triplicate biological and technical replicates. Thermal  
254 cycling parameters consisted of an activation step at 50°C for 2 min, a denaturation step at  
255 95°C for 10 min, and 50 cycles at 95°C for 15 s and 60°C for 1 min. This was followed by  
256 the construction of a dissociation curve through increasing the temperature from 60°C to  
257 95°C at a ramp rate of 2%. A single predominant peak was observed in the dissociation  
258 curve of each gene, supporting the specificity of the PCR product.

#### 259 **Phylogenetic analysis**

260 16S rRNA and functional gene sequences were compared to GenBank nucleotide  
261 and protein databases with the blastn and blastx algorithms (47).

262 The nucleotide sequences of *rpsC*, *proC*, and 16S rRNA genes amplified from the  
263 uranium-contaminated aquifer have been deposited in the GenBank database under  
264 accession numbers FJ042710-FJ042726.

#### 265 **Results and Discussion**

##### 266 **Identification of growth rate related genes with microarray analysis.**

267 *G. uraniireducens*, an isolate from the Rifle study site, is closely related to  
268 *Geobacter* species that predominate during *in situ* uranium bioremediation at the site  
269 (30). Whole-genome scale data on transcript abundance during growth with fumarate as

270 the electron acceptor versus growth on natural Fe(III) oxides in sterile subsurface  
271 sediments (20) or laboratory-synthesized Fe(III) and Mn(IV) oxides is available (GEO  
272 data series GSE10920 and GSE12874). At its optimal temperature of 30°C, *G.*  
273 *uraniireducens* grew faster with fumarate provided as the electron acceptor than with  
274 Fe(III) or Mn(IV) oxides, and even slower in sediments (Table 1).

275 A number of genes involved in protein synthesis had significantly lower transcript  
276 abundance at the slower growth rates (Supplementary Material Tables S2-S4). Of these,  
277 fifty-two were less abundant under all three slow-growth conditions. Two of these genes,  
278 *rpsC* and *rplL*, which code for ribosomal proteins S3 and L7/L12 (Figure 1) were chosen  
279 for further study because their expression levels have also been shown to be linked to  
280 specific growth rates in other microorganisms (48-50).

#### 281 **Correlation between specific growth rate and transcript abundance.**

282 In order to achieve an even wider range of growth rates, *G. uraniireducens* was  
283 grown at various temperatures with a variety of electron acceptors (sediment Fe(III)  
284 oxides; synthetic Fe(III) or Mn(IV) oxides; or fumarate) (Table 1, Supplementary Figure  
285 S2). Specific growth rates ranged from 0.007 h<sup>-1</sup> to 0.106 h<sup>-1</sup>. The specific growth rate  
286 of *G. uraniireducens* increased with temperature in fumarate-grown cultures, but this  
287 same increase was not observed in sediment-grown cells. The fact that growth was  
288 slower in sediment cultures grown at 30°C suggests that some factor other than  
289 temperature, possibly the need to search for Fe(III) oxide sources (51) can limit growth in  
290 sediments. The decrease in specific growth rate in sediments observed at 37 °C can be  
291 explained by the fact that this temperature is above *G. uraniireducens*' optimal growth  
292 range (30).

293           Despite the variety of growth conditions, the number of mRNA transcripts from  
294 both genes normalized against the number of *proC* transcripts (Table 1) was directly  
295 correlated with specific growth rate (Figure 2). The correlation between *rpsC/proC* and  
296 specific growth rate was much better than it was for *rplL/proC* versus specific growth  
297 rate (Figure 2).

298           The specific growth rate of *G. uraniireducens* could also be manipulated by  
299 controlling the availability of ammonium. Addition of ammonium to cultures that were  
300 previously growing under nitrogen-fixing conditions greatly accelerated the specific  
301 growth rate (Figure 3A). Increased growth was associated with a dramatic increase in  
302 *rpsC* transcript abundance (Figure 3B). Under nitrogen-fixing conditions the specific  
303 growth rate was approximately  $0.017 \text{ h}^{-1}$  which, according to the equation from Fig. 2A  
304 ( $y=511x-5.3$ ), should yield a normalized transcript abundance value of 3.5 and compares  
305 well with the value of 3.6 that was observed. These results further suggested that the  
306 abundance of *rpsC* could be used to estimate specific growth rates of *G. uraniireducens*  
307 under changing environmental conditions.

#### 308 **Evaluation of *in situ* specific growth rate in the subsurface.**

309           The 2010 *in situ* uranium bioremediation field experiment conducted in Rifle  
310 provided an excellent opportunity to determine whether the abundance of *rpsC* transcripts  
311 might be a good indicator of the relative specific growth rates of *Geobacteraceae* species  
312 in the subsurface. As previously observed in acetate-amendment studies at the site (26,  
313 31), the addition of acetate resulted in an accumulation of Fe(II) (Figure 4A) and an  
314 increase in the number of *Geobacteraceae* species (Figure 4B), consistent with the  
315 expected stimulation of dissimilatory metal reduction. In contrast to the increase in

316 *Geobacteraceae* species, there appeared to be little net growth of other microorganisms;  
317 as cells labeled with *Geobacteraceae*-specific probes accounted for most of the increase  
318 in cells that was detected with DAPI staining (Figure 4B). The relative abundance of  
319 *Geobacteraceae* species estimated from analysis of 16S rRNA gene sequences further  
320 confirmed the specific stimulation of the growth of *Geobacteraceae* species (Figure 4C  
321 and Supplementary Material Table S5). The majority of 16S rRNA gene sequences  
322 recovered from the samples after day 9 were *Geobacteraceae* species, specifically  
323 *Geobacter bemidjensis* (Supplementary Material Tables S5 and S6), indicating that the  
324 *Geobacteraceae* enumerated with FISH probes were primarily from the genus *Geobacter*.  
325 When acetate concentrations in the subsurface started to decline after day 21, Fe(II)  
326 concentrations also went down and this was accompanied by a decrease in the number of  
327 *Geobacter* cells and their abundance relative to other bacterial species (Figure 4B).

328         Specific growth rates of *in situ* *Geobacter* species were estimated from *rpsC*  
329 transcript abundance. It was assumed that there was a correlation between transcript  
330 abundance of *rpsC* in the subsurface isolate, *G. uraniireducens*, and specific growth rate  
331 of the *in situ* *Geobacter* population (Figure 2A). Specific growth rates for the *in situ*  
332 *Geobacter* species were calculated using the equation in Figure 2A ( $y=511x-5.3$ ) and  
333 ranged from 0.014 to 0.016 h<sup>-1</sup> (Figure 4D). These estimated specific growth rates were  
334 comparable to the specific growth rate of 0.014 h<sup>-1</sup> for *G. uraniireducens* from laboratory  
335 incubations in acetate-amended sediments.

336         Estimated specific growth rates increased 45% with the addition of acetate,  
337 plateaued around day 9, and then started to decline around day 20 to a rate near that  
338 observed when acetate amendments were first started (Figure 4D). This same trend was



339 observed when *Geobacter* cell numbers were monitored over time with FISH.  
340 Immediately following the addition of acetate there was a dramatic increase in cell  
341 numbers up to day 9 (Figure 4D). Assuming logarithmic growth, the increase in cell  
342 numbers in the first 9 days ( $9.11 \times 10^5$  cells/ml) yielded a specific growth rate of 0.0148  
343  $\text{h}^{-1}$ , which is comparable to the maximum specific growth rate estimated by *rpsC*  
344 transcript numbers during this period (Figure 4D). Between days 9 and 20, the rate of  
345 *Geobacter* cell number increase was noticeably slower. The estimated specific growth  
346 rate from cell numbers during this phase was  $0.0006 \text{ h}^{-1}$ , much lower than the specific  
347 growth rates of 0.015-0.016  $\text{h}^{-1}$  estimated from *rpsC* transcript abundance. After day 20,  
348 numbers of *Geobacter* in the groundwater started to decline even though the specific  
349 growth rate estimated from *rpsC* transcripts was higher than the specific growth rate at  
350 time zero.

351         A major factor contributing to the discrepancy between estimated specific growth  
352 rates and changes in cell number after day 9 may have been a bloom in protozoa grazing  
353 on *Geobacter* species. Studies at the Rifle site have shown that protozoa become  
354 abundant in the groundwater when dissimilatory metal reduction is stimulated by the  
355 addition of acetate (Holmes et al. submitted). The increase in protozoan abundance is  
356 significant because protozoa can exploit substantial quantities of bacterial biomass  
357 production (52) and grazing can significantly stimulate microbial metabolic activity and  
358 growth (53, 54).

359         Another consideration is that as Fe(III) oxides are depleted at the Rifle site, the  
360 *Geobacter* populations shift from one that is ca. 90 % planktonic to one in which most of  
361 the cells attach to the sediments (Dar, S. manuscript submitted). The continued decline in

362 the number of planktonic *Geobacter* cells during the later phases of the field experiment  
363 may reflect this. Furthermore, there may be other factors contributing to cell loss. The  
364 estimated *Geobacter* specific growth rates prior to acetate additions were ca. 70% of the  
365 maximum estimated specific growth rates during acetate additions, yet cell numbers were  
366 relatively low. Estimates of growth rate in the subsurface are likely to represent an  
367 average of a wide range of growth rates of cells exposed to different microenvironments  
368 as previously noted in biofilms (55).

### 369 **Implications**

370 These results suggest that monitoring expression of *rpsC* can provide insight into specific  
371 growth rates of subsurface *Geobacter* species, even under situations where predation is  
372 equal or higher than production of new cells. The ability to estimate specific growth rates  
373 in the subsurface during the bioremediation of metals is particularly important, because  
374 the goal may not always be to maximize the specific growth rate or even the overall rate  
375 of metal reduction. For example, it may be desirable to maintain an active but slowly  
376 respiring population of *Geobacter* species that will effectively reduce U(VI) as it enters  
377 the acetate injection zone, without rapidly depleting the Fe(III) oxides needed to maintain  
378 their growth in the subsurface.

379 The approach described here may also be useful for monitoring the growth of  
380 *Geobacter* species in a diversity of other environments in which they play an important  
381 role including anaerobic soils and sediments (18), electrodes harvesting current (56), and  
382 some methanogenic environments (18). It seems likely that a similar approach may also  
383 be useful for monitoring the growth of other subsurface microorganisms, such as the  
384 *Dehalococcoides* species involved in reductive dechlorination (57), or to monitor the

385 growth of microorganisms added to the subsurface to promote bioremediation (58-60).  
386 Furthermore, as the ability to predictively model the growth of subsurface  
387 microorganisms at the genome-scale advances (16, 17, 61-63), it will be increasingly  
388 important to have better methods for monitoring key aspects of microbial physiology,  
389 such as growth rate for model validation.

390

391

### 392 **Figure Legends**

393 Figure 1. Microarray results from experiments comparing three different  
394 experimental conditions (*G. uraniireducens* cells grown with Rifle  
395 sediment, Fe(III) oxide, or Mn(IV) oxide provided as the electron  
396 acceptor) to the control condition (*G. uraniireducens* cells grown with  
397 fumarate provided as the electron acceptor) (p value cutoff  $\leq 0.01$ ).  
398 Transcript levels for both *rpsC* and *rplL* were significantly down-regulated  
399 in all three microarray experiments (indicated by negative fold change in  
400 the figure). Triplicate biological and duplicate technical replicates were  
401 done for all three microarray experiments.

402 Figure 2. The number of (A) *rpsC* and (B) *rplL* mRNA transcripts normalized  
403 against the number of *proC* mRNA transcripts expressed by *G.*  
404 *uraniireducens* at a wide range of growth rates. Triplicate biological and  
405 technical replicates were done for all specific growth rates.

406 Figure 3. (A) The number of *G. uraniireducens* cells in cultures with acetate (5  
407 mM) provided as the electron donor and fumarate (40 mM) provided as

408 the electron acceptor under nitrogen limiting (no  $\text{NH}_4^+$ ) or non-nitrogen  
409 limiting (4.67 mM  $\text{NH}_4^+$ ) conditions. (B) The number of *rpsC* mRNA  
410 transcripts normalized against the number of *proC* mRNA transcripts  
411 expressed by *G. uraniireducens* cells under nitrogen limiting or non-  
412 nitrogen limiting conditions. Triplicate biological and technical replicates  
413 were done for all samples.

414 Figure 4. Growth of *Geobacteraceae* in response to acetate availability during the  
415 uranium bioremediation field experiment conducted at Rifle in 2010. (A)  
416 Acetate and Fe(II) concentrations in groundwater collected during  
417 uranium bioremediation, (B) Number of *Geobacteraceae* in the  
418 groundwater estimated by direct counts of cells labeled with  
419 *Geobacteraceae*-specific FISH probes and total bacterial cells estimated  
420 with general DAPI staining, (C) Proportion of *Geobacteraceae* in the  
421 groundwater estimated by comparing direct counts of cells labeled with  
422 *Geobacteraceae*-specific FISH probes with general DAPI staining of all  
423 cells versus proportion of *Geobacteraceae* found in 16S rRNA gene clone  
424 libraries, and (D) Number of *Geobacteraceae rpsC* mRNA transcripts  
425 normalized against the number of *proC* mRNA transcripts plotted against  
426 the number of *Geobacteraceae* cells/mL estimated by FISH in the  
427 groundwater. Each point is an average of triplicate determinations, and  
428 error bars represent standard deviations. Growth rate constants ( $\mu$ ) were  
429 calculated from the following equation:  $y = 511.35x - 5.2809$ .

430 Acknowledgements

431 Research at the University of Massachusetts was funded by the Office of Science (BER),  
432 US Department of Energy, Awards no. DE-SC0004080 and DE-SC0004814 and  
433 Cooperative Agreement no. DE-FC02-02ER63446. Additional support for field research  
434 was equally supported through the Integrated Field Research Challenge Site (IFRC) at  
435 Rifle, CO, USA and the Lawrence Berkeley National Laboratory's Sustainable Systems  
436 Scientific Focus Area. The US Department of Energy (DOE), Office of Science, Office  
437 of Biological and Environmental Research funded the work under contract DE-AC02-  
438 05CH11231 (Lawrence Berkeley National Laboratory; operated by the University of  
439 California).

440

#### 441 **References**

- 442 **1. Caron DA, Worden AZ, Countway PD, Demir E, Heidelberg KB. 2009.**  
443 **Protists are microbes too: a perspective. *Isme J* 3:4-12.**  
444 **2. Tuomi P, Kuoppo P. 1999. Viral lysis and grazing loss of bacteria in**  
445 **nutrient- and carbon-manipulated brackish water enclosures. *J Plankton Res***  
446 **21:923-937.**  
447 **3. Fuhrman JA, Azam F. 1982. Thymidine Incorporation as a Measure of**  
448 **Heterotrophic Bacterioplankton Production in Marine Surface Waters -**  
449 **Evaluation and Field Results. *Mar Biol* 66:109-120.**  
450 **4. Baath E. 1998. Growth rates of bacterial communities in soils at varying pH:**  
451 **A comparison of the thymidine and leucine incorporation techniques.**  
452 ***Microbial Ecol* 36:316-327.**  
453 **5. Staley JT, Konopka A. 1985. Measurement of in situ activities of**  
454 **nonphotosynthetic microorganisms in aquatic and terrestrial habitats.**  
455 ***Annual review of microbiology* 39:321-346.**  
456 **6. Fuller ME, Mailloux BJ, Streger SH, Hall JA, Zhang PF, Kovacic WP,**  
457 **Vainberg S, Johnson WP, Onstott TC, DeFlaun MF. 2004. Application of a**  
458 **vital fluorescent staining method for simultaneous, near-real-time**  
459 **concentration monitoring of two bacterial strains in an Atlantic Coastal Plain**  
460 **aquifer in Oyster, Virginia. *Appl Environ Microb* 70:1680-1687.**  
461 **7. Fuller ME, Streger SH, Rothmel RK, Mailloux BJ, Hall JA, Onstott TC,**  
462 **Fredrickson JK, Balkwill DL, DeFlaun MF. 2000. Development of a vital**  
463 **fluorescent staining method for monitoring bacterial transport in subsurface**  
464 **environments. *Appl Environ Microb* 66:4486-4496.**

- 465 8. Breeuwer P, Abee T. 2000. Assessment of viability of microorganisms  
466 employing fluorescence techniques. *Int J Food Microbiol* 55:193-200.
- 467 9. Breeuwer P, Drocourt JL, Rombouts FM, Abee T. 1996. A novel method for  
468 continuous determination of the intracellular pH in bacteria with the  
469 internally conjugated fluorescent probe 5 (and 6-)-carboxyfluorescein  
470 succinimidyl ester. *Appl Environ Microb* 62:178-183.
- 471 10. Yamamoto Y, Shiah FK. 2010. Relationship between cell growth and  
472 frequency of dividing cells of *Microcystis aeruginosa*. *Plankton and Benthos*  
473 *Res* 5:131-135.
- 474 11. Harvey RW, George LH. 1987. Growth Determinations for Unattached  
475 Bacteria in a Contaminated Aquifer. *Appl Environ Microb* 53:2992-2996.
- 476 12. Tsujimura S. 2003. Application of the frequency of dividing cells technique to  
477 estimate the *in situ* growth of *Microcystis* (cyanobacteria). *Freshwater Biol*  
478 48:2009-2024.
- 479 13. Burbage CD, Binder BJ. 2007. Relationship between cell cycle and light-  
480 limited growth rate in oceanic *Prochlorococcus* (MIT9312) and  
481 *Synechococcus* (WH8103) (cyanobacteria). *J Phycol* 43:266-274.
- 482 14. Lovley DR. 2003. Cleaning up with genomics: applying molecular biology to  
483 bioremediation. *Nature reviews. Microbiology* 1:35-44.
- 484 15. Lin B, Westerhoff HV, Roling WF. 2009. How Geobacteraceae may dominate  
485 subsurface biodegradation: physiology of *Geobacter metallireducens* in slow-  
486 growth habitat-simulating retentostats. *Environ Microbiol* 11:2425-2433.
- 487 16. Mahadevan R, Palsson BO, Lovley DR. 2011. In situ to in silico and back:  
488 elucidating the physiology and ecology of *Geobacter* spp. using genome-scale  
489 modelling. *Nature reviews. Microbiology* 9:39-50.
- 490 17. Zhuang K, Izallalen M, Mouser P, Richter H, Risso C, Mahadevan R, Lovley  
491 DR. 2011. Genome-scale dynamic modeling of the competition between  
492 *Rhodospirillum rubrum* and *Geobacter* in anoxic subsurface environments. *Isme J* 5:305-  
493 316.
- 494 18. Lovley DR, Ueki T, Zhang T, Malvankar NS, Shrestha PM, Flanagan KA,  
495 Aklujkar M, Butler JE, Giloteaux L, Rotaru AE, Holmes DE, Franks AE,  
496 Orellana R, Risso C, Nevin KP. 2011. *Geobacter*: The Microbe Electric's  
497 Physiology, Ecology, and Practical Applications. *Adv Microb Physiol* 59:1-  
498 100.
- 499 19. Holmes DE, Nevin KP, Lovley DR. 2004. In situ expression of *nifD* in  
500 *Geobacteraceae* in subsurface sediments. *Appl Environ Microbiol* 70:7251-  
501 7259.
- 502 20. Holmes DE, O'Neil RA, Chavan MA, N'Guessan LA, Vrionis HA, Perpetua  
503 LA, Larrahondo MJ, DiDonato R, Liu A, Lovley DR. 2009. Transcriptome of  
504 *Geobacter uraniireducens* growing in uranium-contaminated subsurface  
505 sediments. *Isme J* 3:216-230.
- 506 21. Mouser PJ, N'Guessan AL, Elifantz H, Holmes DE, Williams KH, Wilkins  
507 MJ, Long PE, Lovley DR. 2009. Influence of Heterogeneous Ammonium  
508 Availability on Bacterial Community Structure and the Expression of  
509 Nitrogen Fixation and Ammonium Transporter Genes during in Situ

- 510 **Bioremediation of Uranium-Contaminated Groundwater. Environ Sci**  
 511 **Technol 43:4386-4392.**
- 512 22. O'Neil RA, Holmes DE, Coppi MV, Adams LA, Larrahondo MJ, Ward JE,  
 513 Nevin KP, Woodard TL, Vrionis HA, N'Guessan AL, Lovley DR. 2008. Gene  
 514 transcript analysis of assimilatory iron limitation in Geobacteraceae during  
 515 groundwater bioremediation. *Environ Microbiol* 10:1218-1230.
- 516 23. N'guessan AL, Elifantz H, Nevin KP, Mouser PJ, Methe B, LWoodard T,  
 517 Manley K, Williams KH, Wilkins MJ, Larsen JT, Long PE, Lovley DR. 2010.  
 518 Molecular analysis of phosphate limitation in Geobacteraceae during the  
 519 bioremediation of a uranium-contaminated aquifer. *Isme J* 4:253-266.
- 520 24. Mouser PJ, Holmes DE, Perpetua LA, DiDonato R, Postier B, Liu A, Lovley  
 521 DR. 2009. Quantifying expression of Geobacter spp. oxidative stress genes in  
 522 pure culture and during in situ uranium bioremediation. *Isme J* 3:454-465.
- 523 25. Holmes DE, Mester T, O'Neil RA, Perpetua LA, Larrahondo MJ, Glaven R,  
 524 Sharma ML, Ward JE, Nevin KP, Lovley DR. 2008. Genes for two  
 525 multicopper proteins required for Fe(III) oxide reduction in Geobacter  
 526 sulfurreducens have different expression patterns both in the subsurface and  
 527 on energy-harvesting electrodes. *Microbiology-Sgm* 154:1422-1435.
- 528 26. Holmes DE, Nevin KP, O'Neil RA, Ward JE, Adams LA, Woodard TL,  
 529 Vrionis HA, Lovley DR. 2005. Potential for quantifying expression of the  
 530 Geobacteraceae citrate synthase gene to assess the activity of Geobacteraceae  
 531 in the subsurface and on current-harvesting electrodes. *Appl Environ*  
 532 *Microb* 71:6870-6877.
- 533 27. Lovley DR, Phillips EJP. 1988. Novel Mode of Microbial Engery  
 534 Metabolism- Organic Carbon Oxidation Coupled to Dissimilatory Reduction  
 535 of Iron or Manganese *Appl Environ Microb* 54:1472-1480.
- 536 28. Nevin KP, Lovley DR. 2000. Lack of production of electron-shuttling  
 537 compounds or solubilization of Fe(III) during reduction of insoluble Fe(III)  
 538 oxide by Geobacter metallireducens. *Appl Environ Microbiol* 66:2248-2251.
- 539 29. Esteve-Nunez A, Rothermich M, Sharma M, Lovley D. 2005. Growth of  
 540 Geobacter sulfurreducens under nutrient-limiting conditions in continuous  
 541 culture. *Environ Microbiol* 7:641-648.
- 542 30. Shelobolina ES, Vrionis HA, Findlay RH, Lovley DR. 2008. Geobacter  
 543 uraniireducens sp nov., isolated from subsurface sediment undergoing  
 544 uranium bioremediation. *Int J Syst Evol Micr* 58:1075-1078.
- 545 31. Anderson RT, Vrionis HA, Ortiz-Bernad I, Resch CT, Long PE, Dayvault R,  
 546 Karp K, Marutzky S, Metzler DR, Peacock A, White DC, Lowe M, Lovley  
 547 DR. 2003. Stimulating the in situ activity of Geobacter species to remove  
 548 uranium from the groundwater of a uranium-contaminated aquifer. *Appl*  
 549 *Environ Microbiol* 69:5884-5891.
- 550 32. Williams KH, Long PE, Davis JA, Wilkins MJ, N'Guessan AL, Steefel CI,  
 551 Yang L, Newcomer D, Spane FA, Kerkhof LJ, McGuinness L, Dayvault R,  
 552 Lovley DR. 2011. Acetate Availability and its Influence on Sustainable  
 553 Bioremediation of Uranium-Contaminated Groundwater. *Geomicrobiol J*  
 554 28:519-539.

- 555 33. Lovley DR, Stolz JF, Nord GL, Phillips EJP. 1987. Anaerobic Production of  
556 Magnetite by a Dissimilatory Iron-Reducing Microorganism. *Nature*  
557 330:252-254.
- 558 34. Coates JD, Ellis DJ, Blunt-Harris EL, Gaw CV, Roden EE, Lovley DR. 1998.  
559 Recovery of humic-reducing bacteria from a diversity of environments. *Appl*  
560 *Environ Microb* 64:1504-1509.
- 561 35. Richter H, Lanthier M, Nevin KP, Lovley DR. 2007. Lack of electricity  
562 production by *Pelobacter carbinolicus* indicates that the capacity for Fe(III)  
563 oxide reduction does not necessarily confer electron transfer ability to fuel  
564 cell anodes. *Appl Environ Microb* 73:5347-5353.
- 565 36. Lemke MJ, McNamara CJ, Leff LG. 1997. Comparison of methods for the  
566 concentration of bacterioplankton for in situ hybridization. *J Microbiol Meth*  
567 29:23-29.
- 568 37. Pernthaler J, Glockner FO, Schonhuber W, Amann R. 2001. Fluorescence in  
569 situ hybridization (FISH) with rRNA-targeted oligonucleotide probes.  
570 *Method Microbiol* 30:207-226.
- 571 38. Benjamini Y, Hochberg Y. 1995. Controlling the False Discovery Rate - a  
572 Practical and Powerful Approach to Multiple Testing. *J Roy Stat Soc B Met*  
573 57:289-300.
- 574 39. Postier B, Didonato R, Jr., Nevin KP, Liu A, Frank B, Lovley D, Methe BA.  
575 2008. Benefits of in-situ synthesized microarrays for analysis of gene  
576 expression in understudied microorganisms. *J Microbiol Methods* 74:26-32.
- 577 40. Smyth GK. 2004. Linear models and empirical bayes methods for assessing  
578 differential expression in microarray experiments. *Stat Appl Genet Mol Biol*  
579 3:Article3.
- 580 41. Smyth GK, Speed T. 2003. Normalization of cDNA microarray data.  
581 *Methods* 31:265-273.
- 582 42. Holmes DE, Chaudhuri SK, Nevin KP, Mehta T, Methe BA, Liu A, Ward  
583 JE, Woodard TL, Webster J, Lovley DR. 2006. Microarray and genetic  
584 analysis of electron transfer to electrodes in *Geobacter sulfurreducens*.  
585 *Environ Microbiol* 8:1805-1815.
- 586 43. Holmes DE, O'Neil RA, Vrionis HA, N'Guessan LA, Ortiz-Bernad I,  
587 Larrahondo MJ, Adams LA, Ward JA, Nicoll JS, Nevin KP, Chavan MA,  
588 Johnson JP, Long PE, Lovley DR. 2007. Subsurface clade of *Geobacteraceae*  
589 that predominates in a diversity of Fe(III)-reducing subsurface  
590 environments. *Isme J* 1:663-677.
- 591 44. Eden PA, Schmidt TM, Blakemore RP, Pace NR. 1991. Phylogenetic Analysis  
592 of *Aquaspirillum-Magnetotacticum* Using Polymerase Chain Reaction-  
593 Amplified 16s Ribosomal-Rna-Specific DNA. *Int J Syst Bacteriol* 41:324-325.
- 594 45. Lane DJ, Pace B, Olsen GJ, Stahl DA, Sogin ML, Pace NR. 1985. Rapid-  
595 Determination of 16s Ribosomal-Rna Sequences for Phylogenetic Analyses. *P*  
596 *Natl Acad Sci USA* 82:6955-6959.
- 597 46. Amann RI, Binder BJ, Olson RJ, Chisholm SW, Devereux R, Stahl DA. 1990.  
598 Combination of 16s Ribosomal-Rna-Targeted Oligonucleotide Probes with  
599 Flow-Cytometry for Analyzing Mixed Microbial-Populations. *Appl Environ*  
600 *Microb* 56:1919-1925.



- 601 47. Altschul SF, Gish W, Miller W, Myers EW, Lipman DJ. 1990. Basic Local  
602 Alignment Search Tool. *J Mol Biol* 215:403-410.
- 603 48. Huang SC, Panagiotidis CA, Canellakis ES. 1990. Transcriptional Effects of  
604 Polyamines on Ribosomal-Proteins and on Polyamine-Synthesizing Enzymes  
605 in *Escherichia-Coli*. *P Natl Acad Sci USA* 87:3464-3468.
- 606 49. Milne AN, Mak WNW, Wong JTF. 1975. Variation of Ribosomal-Proteins  
607 with Bacterial-Growth Rate. *J Bacteriol* 122:89-92.
- 608 50. Sarmientos P, Cashel M. 1983. Carbon Starvation and Growth Rate-  
609 Dependent Regulation of the *Escherichia-Coli* Ribosomal-Rna Promoters -  
610 Differential Control of Dual Promoters. *P Natl Acad Sci-Biol* 80:7010-7013.
- 611 51. Childers SE, Ciuffo S, Lovley DR. 2002. *Geobacter metallireducens* accesses  
612 insoluble Fe(III) oxide by chemotaxis. *Nature* 416:767-769.
- 613 52. Fenchel T. 1982. Ecology of Heterotrophic Microflagellates .2. Bioenergetics  
614 and Growth. *Mar Ecol-Prog Ser* 8:225-231.
- 615 53. Biagini GA, Finlay BJ, Lloyd D. 1998. Protozoan stimulation of anaerobic  
616 microbial activity: enhancement of the rate of terminal decomposition of  
617 organic matter. *Fems Microbiol Ecol* 27:1-8.
- 618 54. Strauss EA, Dodds WK. 1997. Influence of protozoa and nutrient availability  
619 on nitrification rates in subsurface sediments. *Microbial Ecol* 34:155-165.
- 620 55. Poulsen LK, Ballard G, Stahl DA. 1993. Use of rRNA fluorescence in situ  
621 hybridization for measuring the activity of single cells in young and  
622 established biofilms. *Appl Environ Microbiol* 59:1354-1360.
- 623 56. Lovley DR. 2012. Electromicrobiology. *Annual review of microbiology*  
624 66:391-409.
- 625 57. Lee PKH, Macbeth TW, Sorenson KS, Deeb RA, Alvarez-Cohen L. 2008.  
626 Quantifying genes and transcripts to assess the in situ physiology of  
627 "Dehalococcoides" spp. in a trichloroethene-contaminated groundwater site.  
628 *Appl Environ Microb* 74:2728-2739.
- 629 58. Amos BK, Sung Y, Fletcher KE, Gentry TJ, Wu WM, Criddle CS, Zhou J,  
630 Löffler FE. 2007. Detection and quantification of *Geobacter lovleyi* strain  
631 SZ: Implications for Bioremediation at tetrachloroethene- and uranium-  
632 impacted sites. *Appl Environ Microb* 73:6898-6904.
- 633 59. Aulenta F, Potalivo M, Majone M, Papini MP, Tandoi V. 2006. Anaerobic  
634 bioremediation of groundwater containing a mixture of 1,1,2,2-  
635 tetrachloroethane and chloroethenes. *Biodegradation* 17:193-206.
- 636 60. Major DW, McMaster ML, Cox EE, Edwards EA, Dworatzek SM,  
637 Hendrickson ER, Starr MG, Payne JA, Buonamici LW. 2002. Field  
638 demonstration of successful bioaugmentation to achieve dechlorination of  
639 tetrachloroethene to ethene. *Environ Sci Technol* 36:5106-5116.
- 640 61. Scheibe TD, Mahadevan R, Fang Y, Garg S, Long PE, Lovley DR. 2009.  
641 Coupling a genome-scale metabolic model with a reactive transport model to  
642 describe in situ uranium bioremediation. *Microbial biotechnology* 2:274-286.
- 643 62. Fang Y, Scheibe TD, Mahadevan R, Garg S, Long PE, Lovley DR. 2011.  
644 Direct coupling of a genome-scale microbial in silico model and a  
645 groundwater reactive transport model. *Journal of contaminant hydrology*  
646 122:96-103.

- 647 63. Barlett M, Zhuang K, Mahadevan R, Lovley D. 2012. Integrative analysis of  
648 *Geobacter* spp. and sulfate-reducing bacteria during uranium  
649 bioremediation. *Biogeosciences* 9:1033-1040.  
650  
651

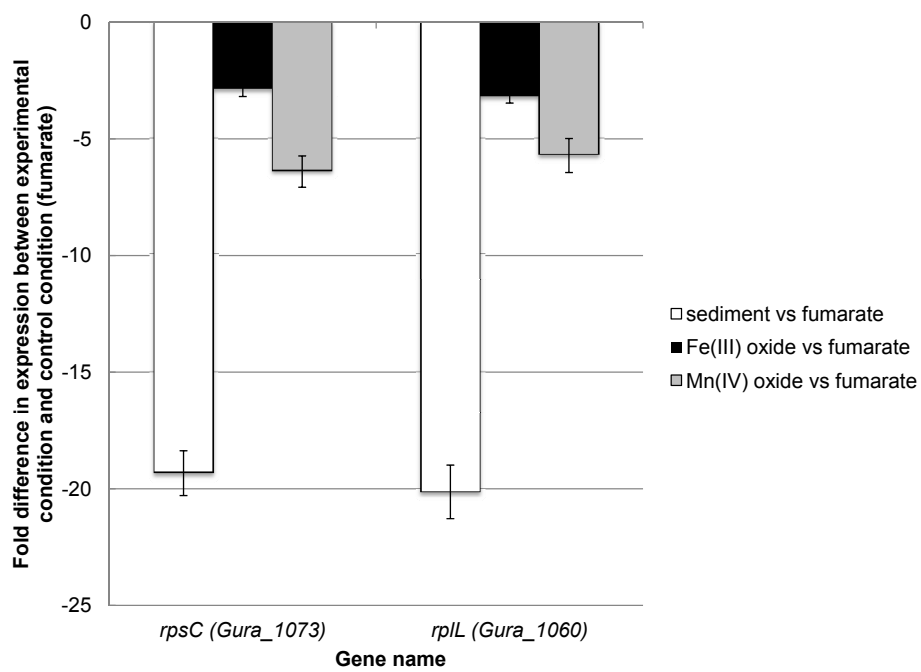


Figure 2

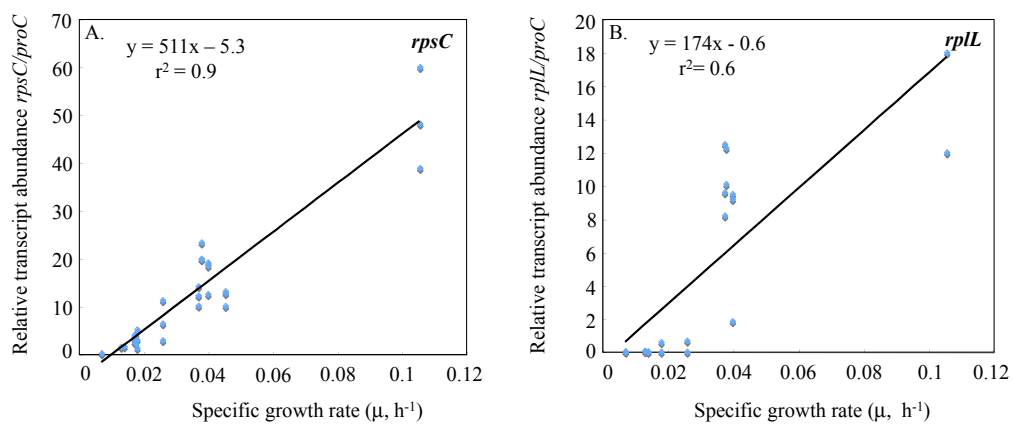
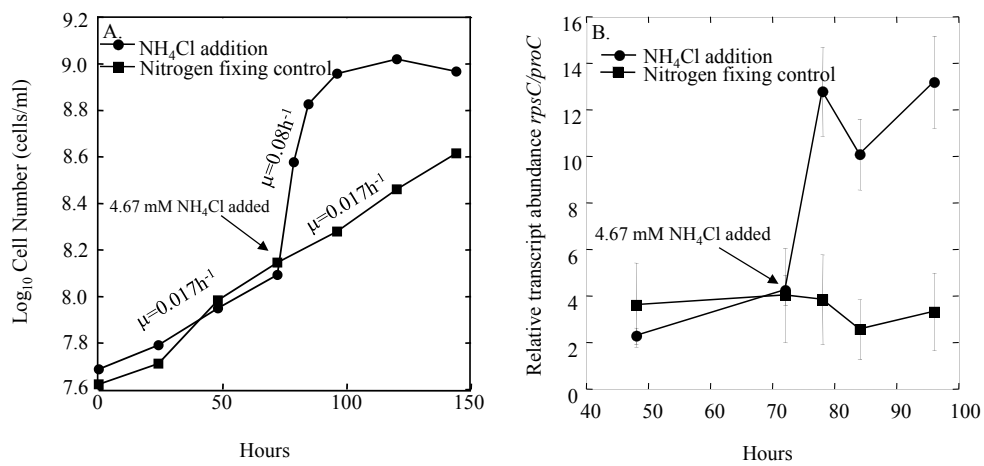


Figure 3



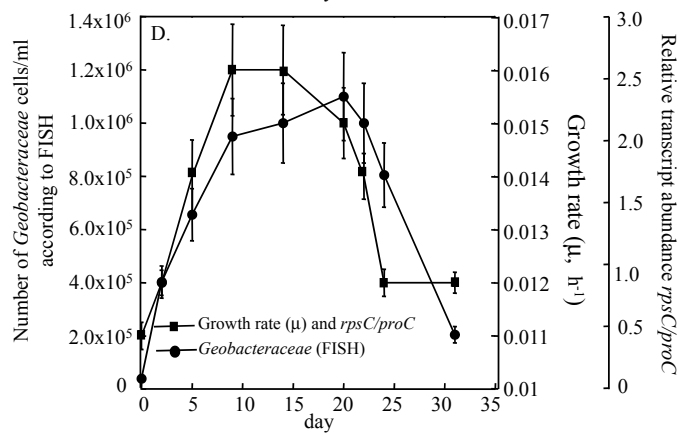
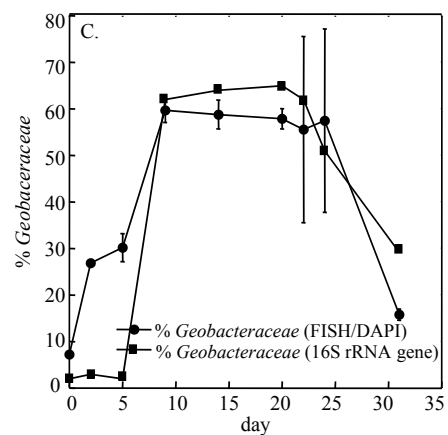
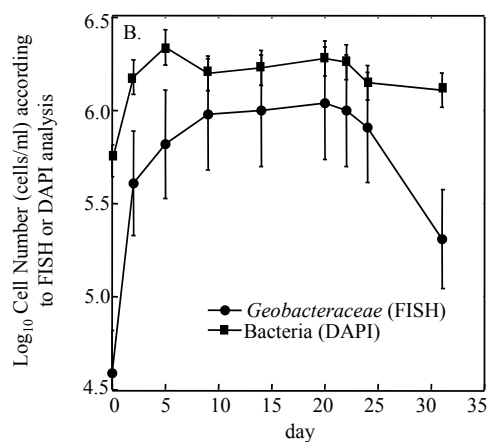
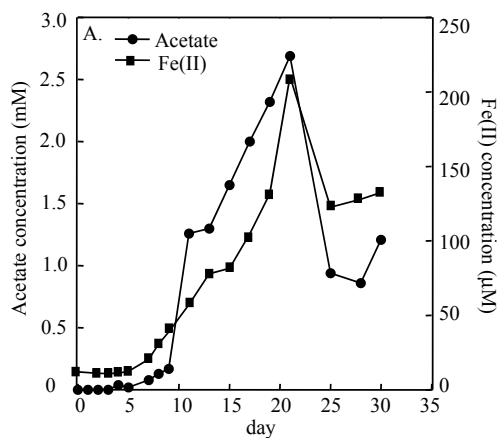


Table 1. Growth rate constants and generation times calculated for *G. waniireducens* cells growing under a variety of conditions. Electron acceptor and/or temperature were varied.

Electron acceptor	Sediment	Sediment	Sediment	Fe(III)-oxide	Mn(IV)-oxide	Fumarate	Fumarate	Fumarate	Fumarate
Growth temperature	18°C	30°C	37°C	30°C	30°C	10°C	15°C	20°C	30°C
Growth rate constant ( $\mu$ , h <sup>-1</sup> )	0.014	0.013	0.007	0.037	0.04	0.018	0.026	0.038	0.106
Doubling time (g, h)	49.50	50.10	89.28	18.50	17.40	38.52	26.72	18.28	6.56
<i>rpsC/proC</i> transcript ratios	1.71 $\pm$ 0.08	1.58 $\pm$ 0.02	0.26 $\pm$ 0.11	12.21 $\pm$ 1.63	16.8 $\pm$ 2.97	3.22 $\pm$ 1.57	6.93 $\pm$ 3.40	28.3 $\pm$ 9.58	55.6 $\pm$ 17.4
<i>rplL/proC</i> transcript ratios	0.17 $\pm$ 0.06	0.04 $\pm$ 0.02	0.30 $\pm$ 0.21	8.18 $\pm$ 6.56	10.9 $\pm$ 6.77	0.02 $\pm$ 0.01	41.9 $\pm$ 40.6	4.34 $\pm$ 2.75	15.3 $\pm$ 2.72